Journal of Digital Contents Society Vol. 16 No. 6 Dec. 2015(pp. 909-916)
http://dx.doi.org/10.9728/dcs.2015.16.6.909

3차원 벡터 필드의 위상 공간 분석

정일홍*, 김용수**

요 약

본 논문에서는 위상 공간 분석을 통해 3D 벡터 필드를 표현하는 방법을 제안한다. 이 방법은 상미분 방정식과 벡터 필드 위상과의 연결에 기초를 두고 있다. 위상 공간 분석은 위상 공간 형태의 자율 방정식 시스템의 기하학적 보간법이 되어야 한다. 이 방정식 시스템의 모든 해는 공간에서의 곡선이 아니라 곡선을 따라가는 점의 움직임과 일치한다. 이러한 분석은 이 논문의 기반이다.

새로운 방법은 3차원 벡터필드에서 육면체 셀을 5 또는 6개의 사면체 셀로 분해하는 것을 요구한다. 임계점은 각 사면체의 간단한 선형 시스템을 풀어서 간단하게 구할 수 있다. 각 사면체의 일반해에 의해 그려지는 전체 곡선과 사면체의 한 면을 포함하는 평면과의 교차점을 계산함으로써 탄젠트 곡선은 구해진다.

키워드 : 위상 공간, 벡터 필드, 일반해, 탄젠트 곡선

The Phase Space Analysis of 3D Vector Fields

Il-Hong Jung*, Yong Soo Kim**

Abstract

This paper presents a method to display the 3D vector fields by analyzing phase space. This method is based on the connections between ordinary differential equations and the topology of vector fields. The phase space analysis should be geometric interpolation of an autonomous system of equation in the form of the phase space. Every solution of it system of equations corresponds not to a curve in a space, but the motion of a point along the curve. This analysis is the basis of this paper.

This new method is required to decompose the hexahedral cell into five or six tetrahedral cells for 3D vector fields. The critical points can be easily found by solving a simple linear system for each tetrahedron. The tangent curves can be integrated by finding the intersection points of an integral curve traced out by the general solution of each tetrahedron and plane containing a face of the tetrahedron.

Keywords : Phase Space, Vector Fields, General Solution, Tangent Curve

1. Introduction

The visualization of 3D vector fields is an important scientific topic because today research in Computational Fluid Dynamics is almost impossible without visualization tools. Computational Fluid Dynamics has widespread applications ranging from oceanic, atmospheric, and astronomical studies to properties of metals under temperature change[1]. However, 3D vector fields are difficult to visualize. The difficulty results from the incapacity of the

※ Corresponding Author : Yong Soo Kim
Received : December 09, 2015
Revised : December 25, 2015
Accepted : December 28, 2015
* Department of Computer Engineering, Daejeon University
Tel: +82-42-280-2548 , Fax: +82-42-280-2889
email: ijung@dju.kr
** Department of Computer Engineering, Daejeon University
Tel: +82-42-280-2547 , Fax: +82-42-280-2889
email: kystj@dju.kr

human visual system to understand displays containing a large number of vectors or curves.

Topological concepts to visualize vector fields ar very powerful. Topology[2][3][4][5] of vector fields consists of critical points and tangents curves connecting these critical points. The power of the topological visualization is that, given the critical points in vector fields and the tangent curves connecting them, one can infer the shape of other tangent curves and hence to some context the structure of the entire set of vector fields. In the conventional topological methods[3][4][5][6], computation of location of critical points can be a rather formidable problem. For example, in the case of curvilinear girds, cells must be searched for possible candidate cells and a nonlinear system of equations must then be solved in order to compute the critical points[3]. The tangent curves are generally calculated using numerical integration over some piecewise interpolant such as Euler's method or Runge-Kutta type method, but these methods produce only approximation to the tangent curves[7].

Our new method is based on the connection between ordinary differential equations and the phase space of vector fields. The connections between differential equations and topology of vector fields were initially developed by Poincare[8][9]. The most important aspects of visualizing vector fields are how to find the critical points and how to integrate the tangent curves. To find the critical points, this new method finds the functions of a velocity vector for each tetrahedron.

We shall analyze a geometrical interpolation of an autonomous system of equations in the form of the phase space of the system[8][9]. This interpolation should be more correctly kinematic interpolation, since every solution of its system of equations corresponds not to a curve in a space, but the motion of a point along the curve. This analysis is the basis of this research.

2. Related Works

2.1 3D Vector Fields Topology

The conventional topological methods are based on critical point theory, which has been widely used to examine solution of ordinary differential equations[8]. They consist of a collection of tangent curves, which separate the flow into regions. Helman and Hesselink [4][5][6] have developed 2D topology software and Globus et al. [3] have developed a tool for visualizing the topology for 3Dl vector fields using critical point classification.

2.1.1 Computation of the Critical Point

Critical points are points where the magnitude of a vector field vanishes. When vector fields are represented over regular grids, critical points can computed by trilinear interpolation for 3Dl vector fields. In the case of curvilinear grids, cell must be searched for possible candidate cells and the simultaneous nonlinear equations must be solved[3]. This normally requires the use of some numerical method, such as Newton's iteration which could possibly fail to converge, or converge to a point which is actually not a critical point [10].

2.1.2 Classification of the Critical Points

If we consider the Taylor's expansion of the fields in the neighborhood of a critical point, then the vector field's local behavior is fully determined by the first order partial derivatives - that is, Jacobian matrix - of the field,

$$\left[\frac{\partial(u,v,w)}{\partial(x,yz)}\right]=\begin{bmatrix}\frac{\partial u}{\partial x} & \frac{\partial u}{\partial y} & \frac{\partial u}{\partial z}\\ \frac{\partial v}{\partial x} & \frac{\partial v}{\partial y} & \frac{\partial v}{\partial z}\\ \frac{\partial w}{\partial x} & \frac{\partial w}{\partial y} & \frac{\partial w}{\partial z}\end{bmatrix}.$$

The eigenvalues and eigenvectors of this matrix determine the local behavior of vector fields around a critical point.

On the basis of the eigenvalues of the Jacobian matrix, Glubus et al.[3] classify a critical point as a node, saddle, or spiral saddle for 3D vector fields. (Figure 1) shows the classification of 3D critical points.

(Figure 1) Classification of 3D critical points

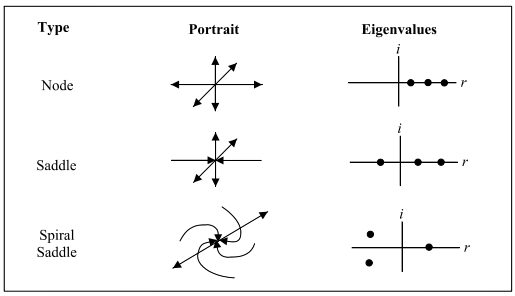

2.1.3. Computation of the Tangent Curves

The tangent curve of a vector field is a curve for which the tangent vector at any point along the curve is parallel to the vector field at that point. In conventional topological methods, tangent curves are generally computed using numerical methods such as Euler's or 4^{th} order Runge-Kutta methods[11] for solving vector-valued initial value problems. Saddle points can be used as the starting points for the tangent curve and the eigenvectors can be used as the starting directions. The end points of the tangent curve are either critical points or points on the boundary of the domain. Because these numerical methods produce only approximations to the tangent curves, some tangent curves may miss a critical point. To solve this problem, when a tangent curve comes very close to a critical point, we simply attach the tangent curve thereto[12][13].

3. The Phase Space Analysis

3.1 Phase Plane Analysis

We consider the linear autonomous system

$$\begin{aligned} x,y) &= \frac{dx}{dt} = a\ x + b_1 y, \\ V(x,y) &= \frac{dy}{dt} = a_2 x + b_2 y, \end{aligned} \qquad (3.1)$$

where $a_1, b_1, a_2,$ and b_2 are constants. The coefficient matrix of constants is nonsingular unless its determinant is $a_1 b_2 - a_2 b_1 = 0$. The system always has a critical point at the origin (0,0) and it has no other singularity.

We look for solutions of equations (3.1) of the form $x = Ae^{tr}$, $y = Be^{tr}$. Substituting for x and y in equations (3.1), we obtain

$$\begin{aligned} (a_1 - r)A + b_1 B &= 0, \\ a_2 A + (b_2 - r)B &= 0. \end{aligned} \qquad (3.2)$$

In order for these two linear homogeneous equations to have a nontrivial solution, it is necessary for the determinant of the coefficients to be zero. Therefore r must be a root of the characteristic equation

$$r^2 + (a_1 + b_2)r + (a_1 b_2 - a_2 b_1) = 0. \qquad (3.3)$$

The roots r_1 and r_2 of equation (3.3) are the eigenvalues of the coefficient matrix of the system (3.1).

Five cases must be considered depending on whether the roots of equation (3.3) have the zero or no nonzero and real roots or complex roots. The five cases are as follows:

Case 1 : $0 \neq r_1 \neq r_2 \neq 0$
Case 2 : $r_1 = 0, r_2 \neq 0$
Case 3 : $r_1 = r_2 = 0$
Case 4 : $r_1 = r_2 \neq 0$
Case 5 : $\mu \pm \lambda i, \lambda \neq 0$

(Figure 2) shows the regions of the above five cases. This figure is generated by varying the value of the vector field at one vertex of the triangle that is marked with white circle and fixing the values of the vector field at the other two vertices, as illustrated by the arrows drawn at these vertices. The interior to the parabolic bounded region is Case 5. The boundary is Case 4, except for the degenerate subcase of Case 3 which is marked by a black box on the boundary. Case 2 consists of a line tangent at this point. The remaining region is Case 1. Not all cases occur with equal frequency. Case 1 and 5 are major cases, while Case 2 and 4 occur much less than Case1 and 5. Case 3 occurs rarely.

(Figure 2) The five case regions

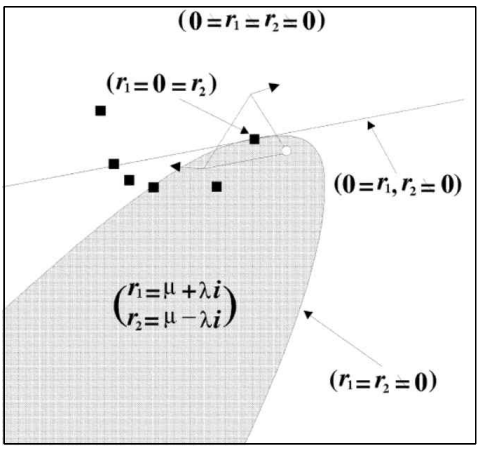

3.2 Phase Space Analysis

Consider the linear autonomous system

$$x,y,z) = \frac{dx}{dt} = a\ x+b_1y+c_1z,$$
$$V(x,y,z) = \frac{dy}{dt} = a_2x+b_2y+c_2z,$$
$$W(x,y,z) = \frac{dz}{dt} = a_3x+b_3y+c_3z, \qquad (3.4)$$

where $a_1, b_1, c_1, a_2, b_2, c_2, a_3, b_3$ and c_3 are constants. We look for solutions of equations (3.4) of the form $x=Ae^{tr}$, $y=Be^{tr}$, $z=Ce^{tr}$. Substituting for x, y, and z in equations (3.4), we obtain

$$(a_1-r)A+b_1B+c_1C=0,$$
$$a_2A+(b_2-r)B+c_2C=0,$$
$$a_3A+b_3B+(c_3-r)C=0. \qquad (3.5)$$

We introduce the characteristic equation

$$-(a_1+b_2+c_3)r^2+(a_1b_2-a_2b_1+a_1c_3-a_3c_1+b_2c_3-b_3c_2)r$$
$$-(a_1b_2c_3+a_2b_3c_1+a_3b_1c_2-a_1b_3c_2-a_2b_1c_3-a_3b_2c_1) \qquad (3.6)$$

with roots r_1, r_2, and r_3. The roots r_1, r_2, and r_3 of equation (3.6) are the eigenvalues of the coefficient matrix of the system (3.3).

Here the characteristic equation is a real cubic equation. Such an equation can have either three real roots or one real and two complex roots, and many different cases occur, depending on the arrangement of th roots r_1, r_2, and r_3. Examining the nonzero multiple roots we find that 4 major cases are possible, as well as 5 degenerate cases which have at least one zero eigenvalues. The nine separate cases follow.

Case 1 : $0 \neq r_1 \neq r_2 \neq r_3 \neq 0$
Case 2 : $0 \neq r_1 \neq r_2 = r_3 \neq 0$
Case 3 : $r_1 = r_2 = r_3 \neq 0$
Case 4 : $r_1 \neq 0, \mu \pm \lambda i, \lambda \neq 0$
Case 5 : $r_1 = 0, 0 \neq r_2 \neq r_3 \neq 0$
Case 6 : $r_1 = r_2 = 0, r_3 \neq 0$
Case 7 : $r_1 = r_2 = r_3 = 0$
Case 8 : $r_1 = 0, r_2 = r_3 \neq 0$
Case 9 : $r_1 = 0, \mu \pm \lambda i, \lambda \neq 0$

(Figure 3) shows the regions of the nine cases. The regions of these degenerate five

cases are represented on a plane which has at least one zero eigenvalue. This plane is called the *zero eigenvalue plane*. The regions of the five degenerate cases on this plane are analogous to the five case regions in the 2D situation as shown in (Figure 2). There exists a surface which contains at least two equal eigenvalues. We call this surface the *equal eigenvalue surface*. The interior to the surface bounded region is Case 4, except for the degenerate subcase of Case 9 on the zero eigenvalue plane. The surface boundary is Case 2, except for the degenerate subcases of Case 7 and 8 on the zero eigenvalue plane and for Case 3 indicated by the curve on the equal eigenvalue surface. The exterior to the surface bounded region is Case 1, except for the degenerate subcases of Case 5 and 6 on the zero eigenvalue plane. This figure represents the three-dimensional analog of (Figure 2).

(Figure 3) The nine case regions

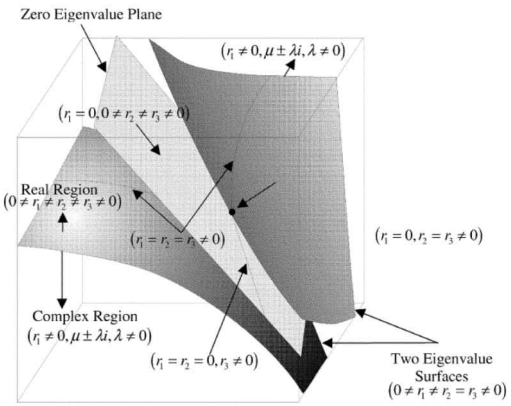

Let us assume that the roots , r_2, and r_3 of equation (3.6) are unequal real roots. We can represent the general solution of equation (3.3) in the following form:

$$x = c_1\alpha_1 e^{r\ t} + c_2\alpha_2 e^{r_2 t} + c_3\alpha_3 e^{r_3 t},$$
$$y = c_1\beta_1 e^{r_1 t} + c_2\beta_2 e^{r_2 t} + c_3\beta_3 e^{r_3 t},$$
$$z = c_1\gamma_1 e^{r_1 t} + c_2\gamma_2 e^{r_2 t} + c_3\gamma_3 e^{r_3 t},$$

where $(\alpha_1,\beta_1,\gamma_1)$, $(\alpha_{21},\beta_2,\gamma_2)$, and $(\alpha_3,\beta_3,\gamma_3)$ are three eigenvectors for r_1, r_2, and r_3.

If three unequal real roots are opposite sign, we classify the critical point as a saddle/saddle/node point. If these roots are same sign, this type of critical point is called a nodal point. (Figure 4) shows the trajectory of the tangent curves in case of three unequal real roots

(Figure 4) The trajectory of the tangent curves in case of three unequal real roots

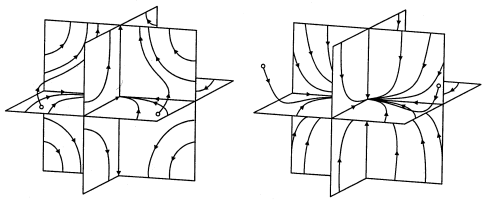

(a) Saddle/saddle//node point (b) nodal point

In case of a real root and complex roots, let us first assume that complex roots are $\mu \pm \lambda i$, and real root is r_1. The general solution of equation (3.3) has form

$$x = c_1\alpha_1 e^{r_1 t} + c_2\alpha_2 e^{(\mu+\lambda i)t} + c_3\alpha_3 e^{(\mu-\lambda i)t},$$
$$y = c_1\beta_1 e^{r_1 t} + c_2\beta_2 e^{(\mu+\lambda i)t} + c_3\beta_3 e^{(\mu-\lambda i)t},$$
$$z = c_1\gamma_1 e^{r_1 t} + c_2\gamma_2 e^{(\mu+\lambda i)t} + c_3\gamma_3 e^{(\mu-\lambda i)t}.$$

If the signs of real root and real part of the complex roos are different, we classify the critical point as a spiral saddle point. If these signs are same, this type of critical point is called a spiral point. (Figure 5) shows the trajectory of the tangent curves in case of a real root and complex roots.

(Figure 5) The trajectory of the tangent curves in case of a real root and complex roots.

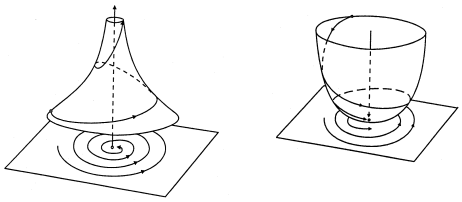

(a) spiral saddle point (b) spiral point

3.3 Tetrahedral Decomposition Method

This new method creates the three dimensional vector field topology by the following algorithm:

1) Decompose hexahedral grid cell into five or six tetrahedral cells.
2) Calculate the coefficient of the linear autonomous system for each tetrahedron.
3) Calculate the coordinate value of the critical points.
4) Classify the critical points.
5) Calculate the eigenvalues of each tetrahedron.
6) Classify each tetrahedron.
7) Compute the general solution for each tetrahedron.
8) Fine the intersection point where the curve, that is traced out by general solution of the tetrahedron, intersects the plane containing a face of a tetrahedron.
9) Integrate the curve
10) Display the three dimensional vector fields topology

4. Performance Evaluation

We present the implementation of the new method for 3D flow data around the an automobile. The 3D data set consists of the coordinate value and the velocity vector value of each grid point on a $4\times64\times64$ curvilinear grid system.

To validation our new method, the method was implemented on a test function. Furthermore, the two conventional methods - Euler's and 4^{th} Order Runge-Kutta method - were also implemented in order to compare our new method's results. The velocity vector of the test function produces a flow which rotates the z axis and spiral inwards. The test function is as follows:

$$u=-0.5x-6y,\quad v=6x-0.5y,\quad w=z-50$$

This function generates the velocity vector values of each grid points in a rectangular Cartesian grid $10\times10\times10$ cells.

A comparison of our new method with the conventional methods is shown in (Figure 6). There are no visual differences between the new method and conventional methods, as shown (Figure 6).

(Figure 6) Validation of proposed method with conventional method

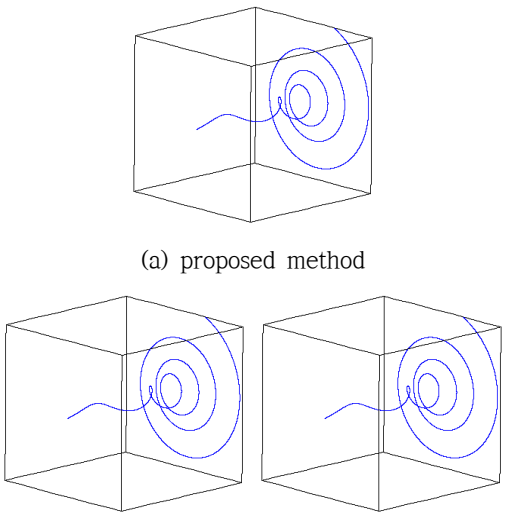

(a) proposed method

(b) Runge-Kutta method (c) Euler's method

(Figure 7) displays the topological graphs around an automobile for 3D flow data.

(Figure 7) 3D vector field topological curves around an automobile

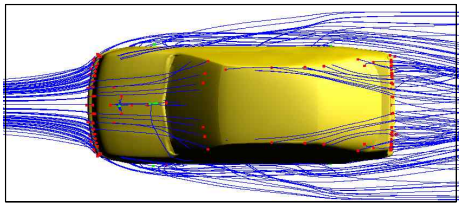

(a) Top View

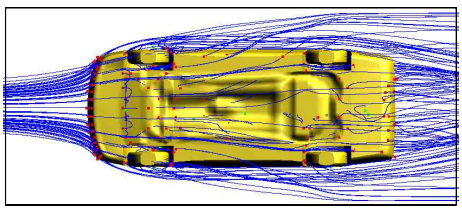

(b) Bottom View

5. Conclusion

The new method for compute the tangent curves using the phase space analysis has been presented. The new method is based on the connections between ordinary differential equations and the phase space of vector fields.

This new method uses functions of the velocity vector for each tetrahedron to find the critical points, while the conventional methods use th bisection method to find the critical points. Thus this new method would reduce the numerical error for finding critical points. Also, this new method has controllable and guaranteed accuracy.

The problem of this research is to find the intersection point of the integral curve, traced out by the general solution of each tetrahedron, and the plane containing a face of the tetrahedron. It is difficult to find exact an intersection point because of numerical error. Further research topics will be development of a more efficient root finding algorithm and extension to separating surface.

References

[1] I. -H. Jung, “A Tetrahedral Decomposition Method for Computing Tangent Curves of 3D Vector Fields”, Journal of Digital Contents Society, Vol.16, No.41, pp.575-581, Aug. 2015.

[2] I. -H. Jung, “An Efficient Visualization Method of Two-Dimensional Vector Fields”, Journal of Korea Multimedia Society, Vol.12, No.11, pp.1623-1628, Nov. 2009.

[3] A. Globus, C. Levit, and T. Lasinski, "A tool for Visualizing the Topology of Three-dimensional Vector Fields," Proc. Visualization '91, IEEE Computer Society, pp.33-40, 1991.

[4] J. L. Helman and L. Hesselink, "Representation and Display of Vector Field Topology in Fluid Data Sets, " IEEE Computer, Vol.22, No.8, pp.27-36, Aug. 1989.

[5] J. L. Helman and L. Hesselink, "Surface Presentation of Two- and Three-Dimensional Fluid Flow Topology," Proc. Visualization '90, IEEE Computer Society, pp.6-13, 1990.

[6] J. L. Helman and L. Hesselink, "Visualizing Vector Field Topology in Fluid Flows," IEEE Computer Graphics and Applications, Vol.11, pp.36-46, May 1991.

[7] J. C. Kim, K. O. Kim, E. K. Kim and C. Y. Kim, "3D Visualization System for Realtime Environmental Data", Journal of Digital Contents Society, Vol.9, No.4, pp.707-715, Dec. 2008.

[8] V. I. Arnold, “Ordinary Differential Equations”, MIT Press, 1973.

[9] S. Birkhoff and G. Rota, “Ordinary Differential Equations”, fourth edition, Wiley, NewYork, 1989.

[10] G. M. Nielson, I. -J. Jung, N. Srinivasan, J, Sung and J. -B. Yoon, "Tools for Computing Tangent Curves and Topological Graphs for Visualizing Piecewise Linearly Varying Vector Fields over Triangulated Domains," in: Scientific Visualization: Overview,

Methodologies and Techniques, G. Nielson, H. Hagen and H. Muller, editors, IEEE Computer Society Press, Los Alamitos, CA, pp.527-562, 1997.

[11] W. H. Press, S. A. Teukolsky, W. T. Vetterlin, and B. P. Flannery, “Numerical Recipes in C: The Art of Scientific Computing”, Second Edition, Cambridge University Press, Cambridge, 1992

[12] G. M. Nielson, "Visualization in Scientific and Engineering Computation," IEEE Computer, Vol.24, No.9, pp.58-66, 1991.

[13] G. M. Nielson and A. Kaufman, "Visualization Graduates," IEEE Computer Graphics and Applications, Vol.14, No. 5, pp.17-18, Sep. 1994.

[14] S. -K. Ueng, C. Sikorski, and K.-L Ma, "Efficient Streamline, Streamribbon, and Streamtube Constructions on Unstructured Grids," IEEE Transactions of Visualization and Computer Graphics, Vol.2, No.2, pp.100-108, Jun. 1996.

정 일 홍

1993년: 애리조나 주립대학 컴퓨터 공학과 졸업 (공학석사)
1998년: 애리조나 주립대학 컴퓨터 공학과 졸업 (공학박사)

1998년 ~ 현 재 : 대전대학교 컴퓨터공학과 교수
관심분야 : 컴퓨터 그래픽스(Computer Graphics), 멀티미디어(Multimedia), 디지털 콘텐츠(Digital Contents), 가상현실(Virtual Reality), 애니메이션(Animation) 등

김 용 수

1981년 : 연세대학교 전기공학과 졸업(공학사)
1983년 : KAIST 전기 및 전자공학과 졸업(공학석사)
1993년 : Dept. of Electrical Eng., Texas Tech Univ. (공학박사)

1983년~1986년 : 삼성전자 종합연구소 주임연구원
1995년~현재 : 대전대학교 컴퓨터공학과 교수
관심분야 : 신경회로망(Neural Networks), 영상처리(Image Processing), 퍼지 논리(Fuzzy Logic), 침입탐지 시스템(Intrusion Detection Systems), 패턴인식(Pattern Recognition), 등